

# Mechanical and Thermal Behaviors of Polypropylene - Multi-Walled Carbon Nanotube Nanocomposite Monofilaments

Department of Textile Engineering,  
Istanbul Technical University,  
Istanbul, Turkey  
E-mail: ersoyemelm@itu.edu.tr

## Abstract

*In this work, multi-walled carbon nanotube (MWCNTs) reinforced polypropylene (PP) monofilaments were prepared by the melt extrusion method. The effect of MWCNTs on the mechanical behaviour of nanocomposite monofilaments was studied by tensile testing and dynamic mechanical analysis (DMA) to understand the mechanism in both the elastic and plastic regions. The results obtained from tensile tests showed that incorporating MWCNTs reduced the tensile strength but increased the Young Modulus of the PP. The Young modulus of the nanocomposite was greatly enhanced to 4587 MPa, compared to 3987 MPa for pristine PP. DMA results are compatible with tensile test results. Thermal analysis showed that the crystallization temperature ( $T_p$ ), melting temperature ( $T_m$ ) and degradation temperatures ( $T_d$ ) are increased by about 15, 2.5, and 8 °C, respectively, with the addition of MWCNTs. Scanning electron microscopy (SEM) observations of the cross section of the nanocomposite monofilaments showed good dispersion of the MWCNTs in the PP matrix.*

**Key words:** nanocomposite monofilament, polypropylene, carbon nanotubes, mechanical properties, dynamic mechanical analysis, thermal stability.

## Introduction

Polypropylene (PP) is a semicrystalline, engineering thermoplastic. PP is extremely widely used in composite fabrication because of its good balance between properties and cost as well as its easy processability and low density [1, 2]. PP is generally modified with nanoparticles to fabricate high performance PP engineering plastics which offer high mechanical and thermal properties [2]. A wide choice of nanoscaled organic/inorganic nanoparticles, such as carbon nanotubes (CNTs), carbon nanofibres, fullerenes, clay, talc, titanium dioxide, etc. are mixed up with polymers to produce nanocomposites with desired properties [2, 3]. Since their discovery in 1991 [4], carbon nanotubes (CNTs) have attracted tremendous research interest due to their extraordinary mechanical, electronic, thermal, and chemical properties [1, 2, 5, 6]. Both experimental and theoretical studies have revealed that CNTs have these exceptional properties [1, 7, 8]. Carbon nanotubes can be used in a wide range of applications, such as chemical sensing, drug delivery and nanoelectronics [9].

Despite the promising potential of CNTs, difficulties have been encountered in exploiting their many impressive fundamental properties due to the irregular dispersal of CNTs within the polymer matrix [2]. In a polymer matrix, filler dispersion and orientation are essential to achieve optimal property improvements. Researchers have used many different techniques to attempt to disperse nanotubes in polymer matrices, including

*in situ* polymerisation, and melt processing [10, 11]. The aim of this work was to study the effect of nanotube content on mechanical, thermal, thermomechanical, and structural properties of PP-Multi Walled Carbon Nanotube (PP-MWCNT) nanocomposite monofilaments obtained via the melt extrusion method.

## Experimental

### Materials

Polypropylene homopolymer resin intended for fibre applications was supplied by the Borealis Company, with the trade name of HG245FB. The melt flow index of PP is defined as 26 g·10 min<sup>-1</sup> at 230 °C in the data sheet [Borealis Co. 2010]. Onset, peak and end temperatures in melting were determined as 155, 161 and 169 °C, respectively, by DSC measurement. Maleic anhydride grafted polypropylene (PP-g-MAH) was used as a compatibiliser, which was supplied by Sigma Aldrich, with the trade name of SA427845. A density of 934 kg·m<sup>-3</sup>, melting point of 156 °C, and viscosity of 4.0 poise at 190 °C were the listed properties of PP-g-MAH.

A masterbatch of PP-MWCNT, containing 11.75% MWCNTs (determined by thermogravimetric analysis), was obtained from the Nanocyl® Company, which was suitable for extrusion with a melting point of 165 °C. The diameter and length of thin MWCNTs used in the master batch preparation were 9.5 nm and 1500 nm on average, respec-

tively, and their BET surface area was 250 - 300 m<sup>2</sup>·g<sup>-1</sup> [Nanocyl Co. 2010].

### Preparation of PP-MWCNT Nanocomposite Monofilaments

PP homopolymer, PP-g-MAH and PP-MWCNT masterbatches were compounded at three different ratios using a laboratory scale double screw melt extruder - DSM Xplore. A three step compounding process was applied to obtain a uniform distribution of carbon nanotubes. At the first and second compounding steps, components were mixed for 15 min. at a 50 r.p.m screw speed and for 15 min. at an 80 r.p.m screw speed, respectively. The temperatures from the feed to spinneret zone were set at 180 - 190 - 200 °C during these two compounding steps. Then the last compounding was applied for 30 min. at an 80 r.p.m screw speed. The temperatures of heating zones were 200 - 210 - 220 °C during the last compounding step. For the extrusion of monofilaments, the screw speed was reduced to 3 r.p.m to achieve an adequate amount of melt exit from the spinneret, which had a diameter of 0.5 mm. The forces applied during extrusion for each sample were changed depending on the viscosity of the polymer - MWCNT blend in order to obtain a 3 r.p.m screw speed. Hence the same amount of material flow from the spinneret in each sample production was achieved. The compounding was run in the 'constant force' mode during extrusion to ensure a constant material flow throughout the extrusion process. 200, 270, 300, and 500 N forces were applied for extrusion

of PP Control, PP1, PP2, and PP3 monofilaments, respectively. All compounding and extrusion processes were performed under Argon atmosphere. After extrusion, the monofilaments passed over two godgets to be subjected to drawing. A draw ratio of 1:6 was applied to all samples by setting the speeds of the first and second godgets at 4.5 m min<sup>-1</sup> and 27.0 m min<sup>-1</sup>, respectively. To ensure a uniform drawing, the temperatures of the first and second godgets were 120 and 60 °C, respectively. Components of the nanocomposite monofilaments and extrusion forces are detailed in **Table 1**.

### Characterisation of PP-MWCNT nanocomposite monofilaments

The breaking stress, tenacity, elongation-at break and Young's modulus of the samples were measured by a James H. Heal Titan<sup>2</sup> universal testing machine according to the BS EN ISO 2062 standard, at a crosshead speed of 250 m min<sup>-1</sup>, maintaining a gauge length of 250 mm and load cell of 120 N. Tests were repeated 10 times for each sample and results evaluated to figure out stress-strain relationships of the nanocomposite monofilaments.

The storage modulus ( $E'$ ), loss modulus ( $E''$ ) and mechanical loss factor ( $\tan \delta = E''/E'$ ) as a function of temperature ( $T$ ) were assessed by dynamic mechanical analysis (DMA) using a Mettler Toledo DMA SDTA861. DMA spectra were taken in the tension mode at 1Hz frequency at ambient temperature and also in a broad temperature range ( $T = -80$  to 120 °C).

The samples were analysed by Thermogravimetric analysis (TGA) using a Seiko TG/DTA 6200 Thermal Analyser under nitrogen flow from 25 to 600 °C at a rate of 10 °C min<sup>-1</sup>. Analyses were carried out with 3.5 mg samples.

The melting and crystallisation behaviour of the nanocomposites were studied under nitrogen atmosphere by differential scanning calorimetry (Perkin Elmer DSC 4000) using a 5 mg sample sealed in aluminum pans. The temperature was raised from -50 to 220 °C at a heating rate of 10 °C min<sup>-1</sup>. After a period of 1 min it was swept back at a -10 °C min<sup>-1</sup> cooling rate.

Scanning electron microscopic (SEM) images were obtained using a Jeol JSM-

**Table 1.** Components of PP-MWCNT monofilaments.

Sample	MWCNT, wt %	CNT Masterbatch, g	PP-g- MAH, g	Pure PP, g
PP Control	0	0	0.196	9.804
PP1	1.84	1.566	0.192	8.242
PP2	4.64	3.949	0.187	5.864
PP3	8.00	6.800	0.180	3.020

**Table 2.** Mechanical properties of the PP-MWCNT nanocomposite monofilaments.

Properties	PP Control	PP1	PP2	PP3
Breaking Strength, N	4.8	3.3	2.8	4.1
Breaking Stress, MPa	259	168	176	162
Elongation at Break, %	45	13	19	25
Young Modulus, MPa	3987	4192	4331	4587
Hook Region Strain, %	0.83	0.85	0.74	0.81
Diameter of Monofilament, mm	0.154	0.157	0.143	0.180
Linear Density, tex	16.2	19.0	14.3	23.2
Tenacity, cN/tex	30	17	20	18

**Table 3.** Isothermal dynamic mechanical properties of the PP-MWCNT nanocomposite monofilaments; storage modulus -  $E'$ ; loss modulus -  $E''$ ; loss factor ( $E''/E'$ );  $\lambda$  = Young modulus.

	PP Control	PP1	PP2	PP3
Maximum storage modulus - $E'_{max}$ , MPa	4734	4735	4813	5078
Corresponding strain, %	0.463	0.489	0.509	0.472
Corresponding tan delta	0.0469	0.0409	0.0600	0.0515
Diameter of Monofilament, mm	0.1394	0.1569	0.1419	0.1825
$E'_{max}$ [PP-MWCNT sample]/ $E'_{max}$ [PP control]	1.00	1.00	1.02	1.07
$\lambda$ [PP-MWCNT sample]/ $\lambda$ [PP control]	1.00	1.05	1.09	1.15

T300 type SEM with a tungsten electron gun with an accelerating voltage capacity of 0.5 – 30 kV. The SEM samples were prepared by freeze cutting in liquid nitrogen and then breaking them. Afterwards they were placed onto the SEM sample holder and sputter-coated with a thin conductive layer of gold.

## Results and discussion

### Mechanical testing of PP-MWCNT nanocomposite monofilaments

Tensile tests of the monofilaments were conducted to determine how mechanical properties were influenced by the presence of MWCNTs. The breaking stress, tenacity, elongation at break, Young's modulus, and linear density of monofilament yarns of all samples are listed in **Table 2**.

**Figure 1** (see page 24) shows a representative set of stress–strain curves for melt drawn monofilament samples at each nanotube concentration. The addition of nanotubes significantly alters the stress–strain behaviour of the fibres.

There are many reasons which may influence the macroscopic mechanical properties of nanocomposites, such as the dispersion, interfacial adhesion, and alignment of CNTs, of which the dispersion of CNTs and CNT-polymer interfacial adhesion are the most important [1, 5]. To make an improvement in mechanical properties, first there should be a high degree of load transfer between the matrix and nanotubes, otherwise the nanotubes behave as holes or nanostructured flaws, inducing local stress concentrations, and the benefits of the CNT properties are lost [8]. Secondly the nanotubes should be well dispersed. If they are poorly dispersed, they will fail by separation of the bundle rather than by failure of the nanotube itself [13, 14].

If we compare the breaking stresses of MWCNT- added samples, that of PP2 is 4.6% higher than that of PP1. Conversely the breaking stress of PP3 sample is 3.2% lower than that of PP1. There is no significant difference between breaking stresses of the samples. Hence it can be concluded that a well dispersed CNT-polymer structure could be formed from

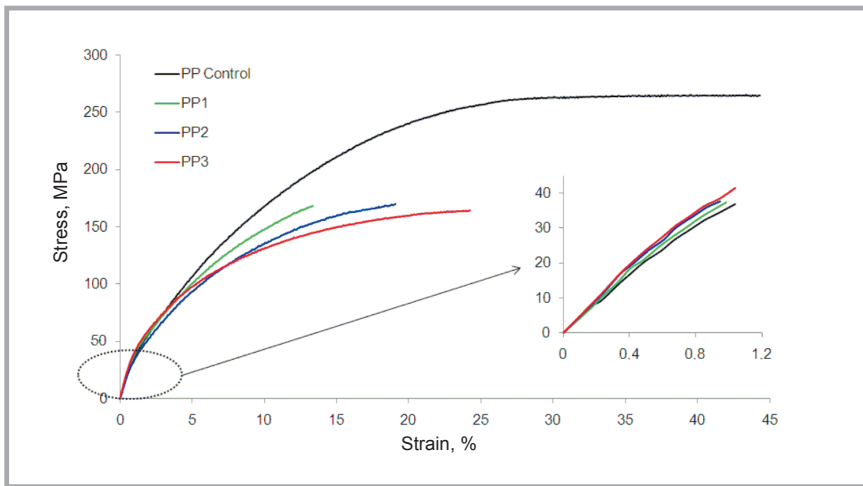


Figure 1. Stress–strain curves for PP-MWCNT monofilaments.

all of the samples. On the other hand it is clear that with the addition of MWCNTs, the level of breaking stress shows a sharp fall, which may be due to the poor interfacial interaction of the MWCNTs with the PP matrix because of the nonpolarity of the MWCNTs and PP [1, 15]. Also, due to the restriction to chain mobility in the composites, stress may be concentrated at the filler–polymer interface, which may develop local crazes and cracks that quickly propagate in three directions, resulting in sample fracture at a relatively low elongation at break [2]. On the other hand the elongation at break increases with the CNT ratio, which means the total interfacial region has a positive effect on the elongation at break.

If we examine the elastic region, in which lower stresses are active at the CNT-polymer interface, the Young modulus increases with the addition of nanotubes (Figure 1). The contribution of the Young modulus of MWCNTs to the total

modulus of nanocomposite monofilament in the elastic region is better than in the plastic region owing to the good adhesion between MWCNTs and the PP matrix. The Young modulus of PP1, PP2 and PP3 monofilaments is 5, 9, and 15% higher than that of PP Control, respectively. These mechanical results indicate that the stiffness of the composite increases with MWCNT content.

#### DMA analyses of PP-MWCNT nanocomposite monofilaments

Isothermal tension experiments showed that the storage modulus tends to increase with MWCNT concentration. The highest storage modulus, 5078 MPa, was obtained for PP3, comprising 8% MWCNT, which was 7% higher than that of PP Control at the same strain level. The MWCNT contents of PP2 and PP3 significantly contributed to the better elastic behaviour of composites. The results of PP1 were the same as PP Control, with a maximum of 4735 MPa. These findings

show great similarities with the Young modulus values obtained in uniaxial tension tests (see Table 3). Due to their competitive elastic modulus, all of PP-MWCNT nanocomposite monofilament samples were found suitable for various technical textile applications where repeated loads are applied at low strain levels, such as electronic textile application as an interlayer in coats, electrostatic protection covers or bags for sensible electronic circuits, etc.

Thermomechanical measurement were also conducted. The storage modulus as well as the  $\tan \delta$  versus temperature traces for the PP-MWCNT monofilaments are shown in Figures 2.a and 2.b. All the curves in Figure 2.a show the same pattern and can be divided in the three main zones: glassy (from  $-80$  to  $-1.51$  °C), glass–rubber transition (from  $-1.5$  to  $68$  °C) and rubbery (from  $68$  to  $120$  °C). Figure 2.b shows the effect of MWCNT on the loss factor ( $\tan \delta$ ) for PP-MWCNT monofilaments. In all three zones the storage modulus ( $E'$ ) of the PP increased with the incorporation of MWCNTs. In addition to an improvement in the storage modulus, the loss factor ( $\tan \delta$ ) is decreased in all zones, which means the elastic recovery behaviour of the monofilaments are improved.

#### Thermal properties of PP-MWCNT nanocomposite monofilaments

##### Differential scanning calorimetry

The DSC analyses give the glass transition, crystallisation and melting temperatures as determined from the exotherm versus temperature curves. Figure 3 shows the crystallisation exotherms of PP-MWCNT nanocomposite monofilaments from DSC. The crystal-

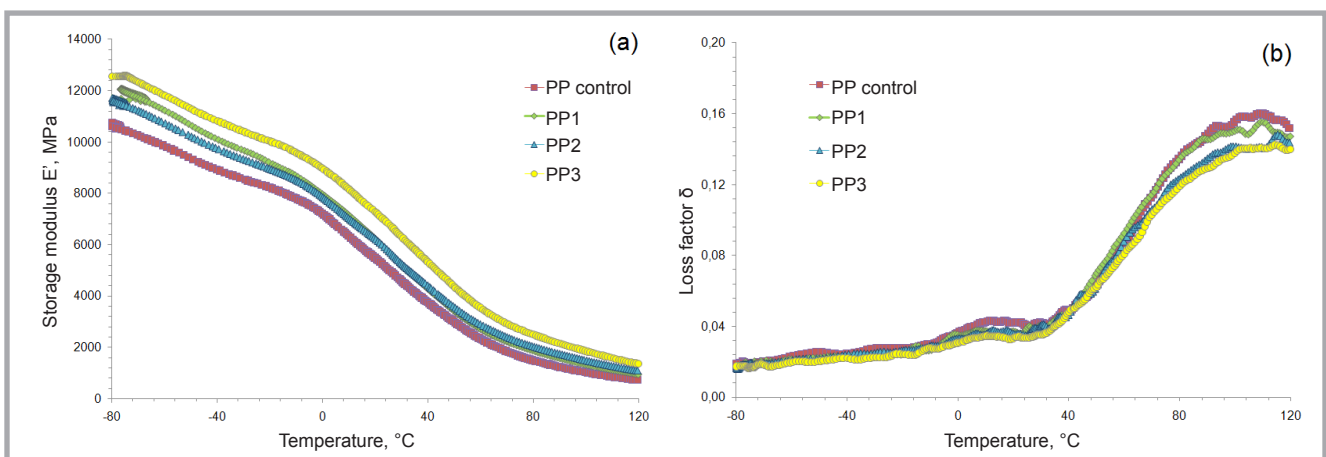


Figure 2. (a) Storage modulus  $E'$  vs temperature curves for PP-MWCNT monofilaments (b) loss factor  $\delta$  vs temperature curves for PP-MWCNT monofilaments.

lisation temperature ( $T_p$ ), defined as the peak temperature of the crystallisation exotherm, the crystallization enthalpy ( $\Delta H_c$ ), the percentage of crystallinity ( $X_c$ ), the temperature at the intercept of the tangents at the baseline and the high-temperature side of the exotherm ( $T_{onset}$ ) were all calculated from DSC curves of the cooling cycle. The melting peak temperature ( $T_m$ ) of the samples was determined from DSC curves of the heating cycle. Results are listed in **Table 4**.

The value of theoretical crystallinity,  $\Delta H_c^0$  was taken to be 209 J/g for 100% crystalline PP [1, 12, 16]. The percentage of crystallinity was determined using **Equation 1** [16, 17].

$$X_c = \frac{\Delta H_c}{\Delta H_c^0(1 - wt\%)} \times 100 \quad (1)$$

where  $1 - wt\%$  is the weight fraction of polymers.

From **Table 4**, it can be seen that  $T_p$  and  $T_m$  of the PP-MWCNT nanocomposite monofilaments with 8 wt% MWCNT content are increased by about 15 and 2.5 °C, respectively. The increase in  $T_p$  of the nanocomposite monofilaments can be explained by nanotubes serving as a nucleating agent for crystals in the nanocomposites, which allows the crystallisation process to occur more easily while the melted nanocomposites are cooling. Thus the crystallization process starts at higher temperatures in MWCNT monofilaments while cooling.

The percentage of crystallinity ( $X_c$ ) of all PP-MWCNT monofilament samples is higher than that of the PP Control monofilament.  $X_c$  of the PP2 monofilament is 44.7%, which means a 5% increase. There is a slight decrease in the  $\Delta H_c$  and  $X_c$  for PP3 sample, which can be ex-

**Table 4.** Characteristic temperatures and enthalpy of crystallisation of PP and PP-MWCNT monofilaments.

Sample	$T_p$ , °C	$T_{onset}$ , °C	$\Delta H_c$ , °C	$X_c$ , %	$T_m$ , °C
PP Control	113.1	116.0	82.9	39.7	162.5
PP1	127.6	130.8	90.1	43.9	165.1
PP2	126.2	129.3	89.1	44.7	164.6
PP3	127.9	130.9	80.7	42.0	164.9

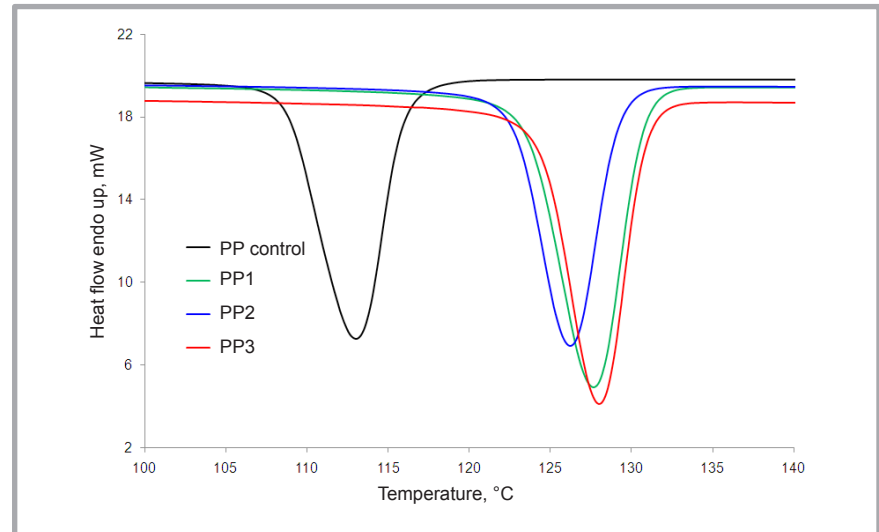


**Figure 3.** DSC crystallisation exotherms of neat PP and PP-MWCNT nanocomposite monofilaments.

plained by the attribution of MWCNTs to the restriction of mobility of the PP molecular chains [12]. Therefore crystalline regions could not be formed in the PP3 sample as much as in the PP1 and PP2 samples.

The increase in  $T_m$  with the filler could be explained by the simplified Thomson–Gibbs equation [2].  $T_m$  increases if the thickness of the lamella increases. Thus MWCNTs act as additional active substrates, promoting thicker lamella of the PP matrix. Moreover MWCNTs reduce the mobility of the PP matrix [1, 2].

#### Thermal gravimetric analysis

TG curves and corresponding derivative curves (DTG) of PP and PP-MWCNT nanocomposite monofilaments are presented in **Figures 4.a** and **4.b**. All samples demonstrated the typical single step degradation behaviour of PP Control monofilament. The sharp fall of the TG curve was hindered with the addition of MWCNTs up to 430 °C. The mass loss rate of the PP Control sample starts to accelerate at around 380 °C, while that of the PP-MWCNT samples starts to accelerate at around 400 °C (**Figure 4.a**).

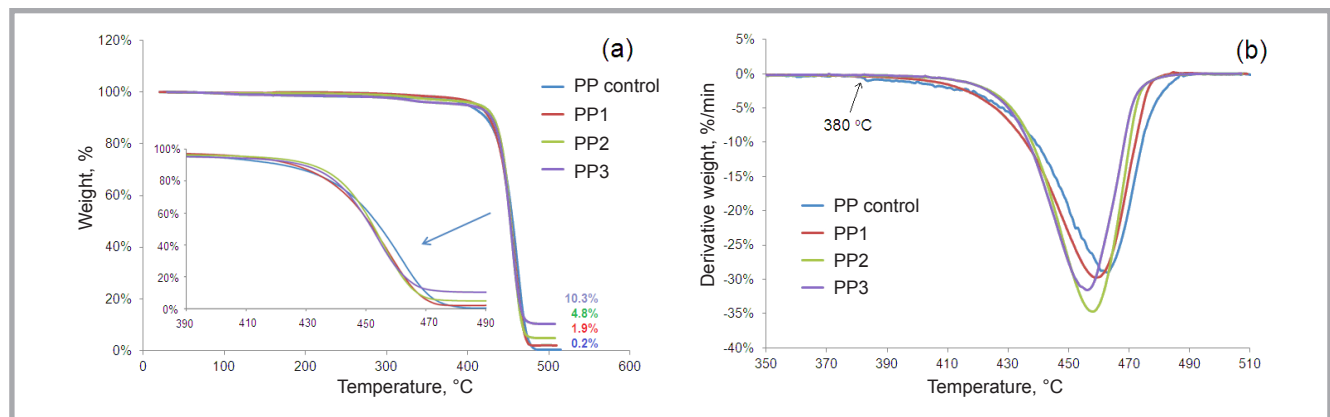


**Figure 4.** Thermogravimetric analysis thermographs of neat PP and PP-MWCNT monofilaments: (a) TG curves and (b) DTG curves.



**Table 5.** Comparison of TG results of PP Control and PP-MWCNT nanocomposite monofilaments.

Sample	Temperature at 10% weight loss, °C	Temperature at 50% weight loss, °C	Max. decomposition temperature, °C	Residual Weight Ratio, wt%
PP Control	422.2	445.0	462.8	0.2
PP1	426.0	452.5	459.0	1.9
PP2	431.9	453.0	458.0	4.8
PP3	429.1	452.1	456.2	10.3

Some specific temperatures are presented in **Table 5**. Temperatures at 10% weight loss of PP-MWCNT monofilaments, which is an indicator of the beginning of the acceleration of decomposition, are 4 – 10 °C higher than that of the PP Control. It is common practice to consider the degradation temperature at 50% weight loss of the sample as an indicator of structural destabilisation. Analysis showed that the PP Control sample is seen to be thermally stable up to 445 °C. An enhancement of around 7 – 8 °C is achieved for PP-MWCNT samples in terms of the degradation temperature. There is a slight decrease in the degradation temperature of the PP3 sample when compared with the PP1 and PP2, which could be explained by the high heat capacity and thermal conductivity of MWCNTs as MWCNTs cause them to reach a higher temperature more quickly than the surrounding matrix. A slight decrease in maximum decomposition temperatures was determined in MWC-

NT-added samples when compared with the PP Control sample, which can be explained by the thermal conductivity of MWCNTs, which becomes significant at higher temperatures.

Residual weight ratios (wt%) at 500 °C are determined as 0.2, 1.9, 4.8, and 10.3% for the PP Control, PP1, PP2, and PP3 samples, respectively. These results show that CNT ratios obtained in the nanocomposite monofilaments conform with the calculated MWCNT ratios in **Table 1**, which means a good distribution was achieved in the nanocomposite monofilament samples.

#### Scanning electron microscopy of PP-MWCNT nanocomposite monofilaments

It is well known that the physical properties of polyolefins are strongly dependent on morphology and structure [1]. Since CNTs have a low bending stiffness and high aspect ratio, they are easy

to agglomerate in a polymer matrix. The morphology and degree of dispersion of MWCNTs in the polypropylene matrix were studied using SEM. **Figures 5** and **6** show a cross section of a cut and broken end of the PP2 nanocomposite monofilament, respectively. The structural integrity throughout the cross section of PP2 clearly appears in the images. Mechanical separation of CNTs from bundles was achieved by melt compounding, with no void at the polymer-CNT interface. It is observed from SEM images that a nanocomposite structure was formed.

#### Conclusion

PP-MWCNT nanocomposite monofilament production by melt extrusion presented in this study is offered as an industrially compatible method. The process conditions are quite suitable for mass production in industry. Mechanical performances in the elastic region of nanocomposite monofilaments were improved. The thermal stability and crystallisation process of the nanocomposite monofilaments were noticeably improved compared to pure PP monofilament. SEM observations of the cross section of the nanocomposite monofilaments showed that the structural integrity and separation of CNTs from bundles were achieved in the PP polymer matrix by

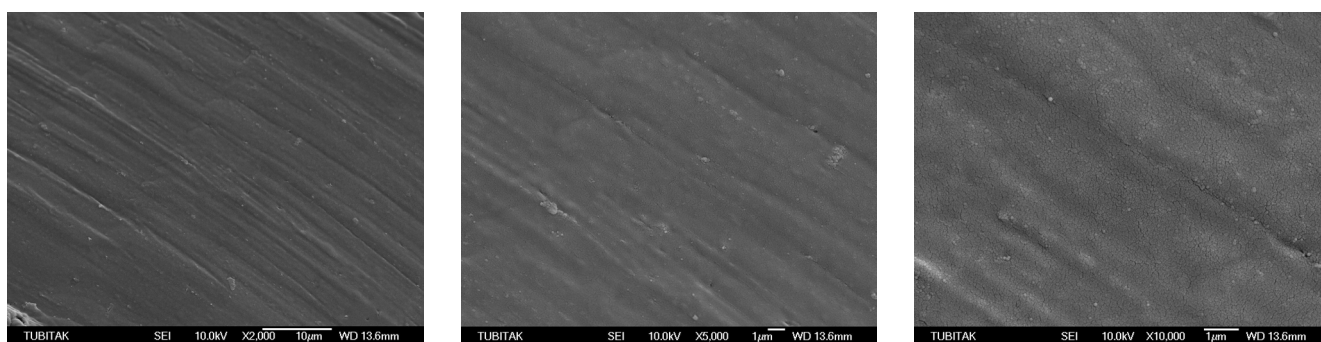


**Figure 5.** SEM micrograph of a cut end of PP2 monofilament at 2000 $\times$ , 5000 $\times$  and 10,000 $\times$  magnification.

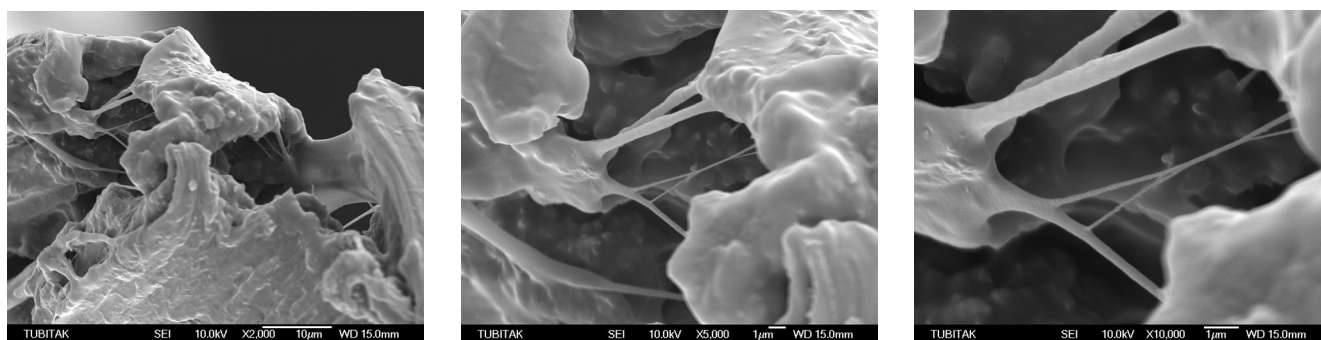


**Figure 6.** SEM micrograph of a broken end of PP2 monofilament at 2000 $\times$ , 5000 $\times$ , and 10,000 $\times$  magnification.

melt compounding. The PP-MWCNT nanocomposite monofilaments developed in this study are favorable for technical textiles that need thermal stability in addition to acceptable tensile properties.

## Acknowledgment

This article was prepared based on the Project TUBITAK MAG 107M126, which was funded by The Scientific and Technical Research Council of Turkey.

## References

1. Fereidoon A, Ghorbanzadeh M, Saedodin A, Saedodin S. *J. Macromol. Sci. Part B: Phys.* 2008; 48: 196–211.
2. Mina MdF, Haque MdA, Bhuiyan MdKH, Gafur MdA, Tamba Y, Asano T. *J. Appl. Polym. Sci.* 2010; 118: 312–319.
3. Winey KI, Du F, Haggemueller R, Kashiwagi T. U.S. Patent 7,265,175, 2007.
4. Iijima S. *Nature* 1991; 354: 56–58.
5. Feng XQ, Shi DL, Huang YG, Hwang KC. *Multiscale in Molecular and Continuum Mechanics: Interaction of Time and Size from Macro to Nano*, Sih GC. Ed. Springer 2007, 103–139.
6. Shokrieh MM, Rafiee R. *Mech. Comp. Mater.* 2010; 46(2): 155–172.
7. Salvétat JP, Bonard JM, Thomson NH, Kulik AJ, Forró L, Benoit W, Zuppiroli L. *Appl. Phys. A*. 1999; 69: 255–260.
8. Lau KT, Hui D. *Carbon* 2002; 40: 1605–1606.
9. Collins PG, Avouris P. *Scientific American* 2000; 283(6): 62–69.
10. Dondero WE, Gorga RE. *J. Polym. Sci. Part B: Polym. Phys.* 2006; 44: 864–878.
11. Ahir SV, Huang YY, Terentjev EM. *Polymer* 2008; 49: 3841–3854.
12. Chow WS, Mohd Ishak ZA, Karger-Kocsis J, Apostolov AA, Ishiaku, U.S. *Polymer* 2003; 44(24): 7427–7440.
13. Harmon JP, Muisener PAO, Clayton L, D'Angelo J, Sikder AK, Kumar A, Meyyanoan M, Cassell AM. *Mater. Res. Society Symposium Proceedings*, Boston, USA, November, 2001; 697: 425–435.
14. Schadler LS, Giannaris SC, Ajayan PM. *Appl. Phys. Lett.* 1998; 73(26): 3842–3844.
15. Vargas AF, Orozco VH, Rault F, Giraud S, Devaux E, López BL. *Composites Part A: Appl. Sci. & Manuf.* 2010; 41: 1797–1806.
16. Tjong SC, Bao SP, Liang GD. *J. Polym. Sci. Part B: Polym. Phys.* 2005; 43: 3112–3126.
17. McNally T, Pötschke P, Halley P, Murphy M, Martin D, Bell SEJ, Brennan GP, Bein D, Lemoine P, Quinn JP. *Polymer* 2005; 46: 8222–8232.



# INSTITUTE OF BIOPOLYMERS AND CHEMICAL FIBRES

## LABORATORY OF ENVIRONMENTAL PROTECTION

The Laboratory works and specialises in three fundamental fields:

### R&D activities:

- research works on new technology and techniques, particularly environmental protection;
- evaluation and improvement of technology used in domestic mills;
- development of new research and analytical methods;

■ **research services** (measurements and analytical tests) in the field of environmental protection, especially monitoring the emission of pollutants;

■ **seminar and training activity** concerning methods of instrumental analysis, especially the analysis of water and wastewater, chemicals used in paper production, and environmental protection in the paper-making industry.

Since 2004 Laboratory has had the accreditation of the Polish Centre for Accreditation No. AB 551, confirming that the Laboratory meets the requirements of Standard PN-EN ISO/IEC 17025:2005.



AB 388

### Investigations in the field of environmental protection technology:

- Research and development of waste water treatment technology, the treatment technology and abatement of gaseous emissions, and the utilisation and reuse of solid waste,
- Monitoring the technological progress of environmentally friendly technology in paper-making and the best available techniques (BAT),
- Working out and adapting analytical methods for testing the content of pollutants and trace concentrations of toxic compounds in waste water, gaseous emissions, solid waste and products of the paper-making industry,
- Monitoring ecological legislation at a domestic and world level, particularly in the European Union.

### A list of the analyses most frequently carried out:

- Global water & waste water pollution factors: COD, BOD, TOC, suspended solid (TSS), tot-N, tot-P
- Halogenoorganic compounds (AOX, TOX, TX, EOX, POX)
- Organic sulphur compounds (AOS, TS)
- Resin and chlororesin acids
- Saturated and unsaturated fatty acids
- Phenol and phenolic compounds (guaiacols, catechols, vanillin, veratrols)
- Tetrachlorophenol, Pentachlorophenol (PCP)
- Hexachlorocyclohexane (lindane)
- Aromatic and polyaromatic hydrocarbons
- Benzene, Hexachlorobenzene
- Phthalates
- Carbohydrates
- Glycols
- Polychloro-Biphenyls (PCB)
- Glyoxal
- Tin organic compounds

### Contact:

INSTITUTE OF BIOPOLYMERS AND CHEMICAL FIBRES  
ul. M. Skłodowskiej-Curie 19/27, 90-570 Łódź, Poland  
Małgorzata Michniewicz Ph. D.,  
tel. (+48 42) 638 03 31, e-mail: michniewicz@ibwch.lodz.pl

Received 11.07.2011 Reviewed 25.06.2012